Properties of Thiol End-Capped and Iodine-Doped Sexithiophene Disulfide Semiconducting Polymers Bridging Nanogap Gold Electrodes

By *Wei Huang,* Hirofumi Tanaka, Takuji Ogawa,** and *Xiao-Zeng You*

Research on supramolecular electronics, for instance, nanosized optoelectronic devices, has attracted much attention recently because self-assembly is an attractive and facile nanofabrication technique for the precise engineering of structures on the nanometer scale and the performance of molecular assemblies that constitute electronic devices is fundamental for research purposes and technical applications.[1–3] In supramolecular electronics, the construction and properties of supramolecular nanosized optoelectronic devices are crucial for investigating nanosized field-effect transistors, photovoltaic devices, light-emitting diodes, and logic gates.

Assemblies of versatile π-conjugated systems on the 5–100 nanometer length scale have been achieved by molecular self-assembly with the aim to fit these organic semiconducting structures between gap electrodes.[4–10] In our previous studies, electropolymerization was used to fabricate oligothiophene-based nanodevices,[11–12] but the conductance of the resulting polymers was relatively low mainly because of the high bandgap of the molecule and the interfacial barrier between the metal and the molecule. Fabricating nanodevices using Au-S bonds between the gold electrodes and the thiol end-capped organic molecules has been proven to be a good strategy to effectively reduce the interfacial barrier.[13–17] On the other hand, the relative conductance of oligothiophenes can be changed by oxidizing or reducing them, or introducing a dopant into the bulk because the oligothiophene proconductors can become oligothiopheniums, which are much better conductors because of the unfilled HOMO and a change in geometry which creates mid-gap states.[18]

Formation of the disulfide bond is an effective way to extend the length of oligothiophenes.[19–21] Compared to oligothiophene polymers, disulfide oligothiophene polymers have worse π-conjugated systems and lower conductance. Nevertheless, the conductivity of polymers can be significantly increased when a dopant is used. In this paper, we used iodine as an oxidant and dopant simultaneously to react with a sexithiophene dithiol having a molecular length of 2.16 nm. As a result, stable thiol end-capped and iodine-doped sexithiophene disulfide semiconducting polymers, whereby the thiol groups are positioned at both ends and the neighboring two sexithiophene units are connected by a sulfur-sulfur bond, were self-assembled in situ and chemisorbed successfully on a pair of facing gold electrodes with a gap of about 20 nm (Scheme SI1). The resistance and interfacial barrier of the resulting nanodevices could be effectively reduced by means of the formation of Au-S bonds between the molecule and the gold electrode as well as the inclusion of an iodine dopant in the oligothiophene chains. Reproducible temperature-dependent current-voltage and current-time curves for these nanodevices were recorded and careful examination of this data shows characteristics of typical semiconducting and photoresponsive nanodevices.

Firstly, we used a Au-coated SiO_2 surface to optimize the experimental conditions of in-situ oxidation, doping, and self-assembly. A typical scanning electron microscopy (SEM) image of the thiol end-capped and iodine-doped sexithiophene disulfide polymer is shown in **Figure 1a**. To obtain this polymer a suitable concentration of 0.5 mmol L^{-1} sexithiophene dithiol and excess iodine in chloroform were used. It was found that part of the polymer was standing, whereas other parts of the polymer were lying on the gold surface forming a cross-linked network structure.[22–24] Tapping-mode atomic force microscopy (TM-AFM) morphological observations for this polymer (Figure 1b) further confirmed the network structure that might be prevailing because of the free rotation and the bond-angle restriction of the S-S and S-C single bonds of the disulfide units in the polymer. The saturated doping ratio of iodine for the sexithiophene disulfide polymer is 1.98 %, which can be deduced from the nitrogen percentage in the presence of an acid-base adduct of $NEt_3 \cdot HI$ in the elemental analysis for the self-assembled polymer.

Then, we used gold electrodes with a nanogap of about 20 nm as the substrate (see FigureS1 in Supporting Information). The gold electrodes were covered with a 100-nm thick Si_3N_4 layer, after the resist and the pads were stripped off from the surface except for the window area that was defined by the Ar^+ beams, to fabricate a nanodevice under suitable experimental conditions. Two Au electrodes facing each other were bridged by the thiol end-capped and iodine-doped sexithiophene disulfide polymers. SEM images of the resulting nanodevice with different

[*] Prof. W. Huang, Prof. X. Z. You
State Key Laboratory of Coordination Chemistry
Nanjing National Laboratory of Microstructures
School of Chemistry and Chemical Engineering
Nanjing University
Nanjing 210093 (P.R. China)
E-mail: whuang@nju.edu.cn
Prof. W. Huang, Dr. H. Tanaka, Prof. T. Ogawa
Research Center for Molecular-Scale Nanoscience
Institute for Molecular Science
National Institutes of Natural Sciences
5-1 Higashiyama, Myodaiji-cho, Okazaki, Aichi, 444-8787 (Japan)
E-mail: ogawa@chem.sci.osaka-u.ac.jp
Dr. H. Tanaka, Prof. T. Ogawa
Department of Chemistry, Graduate School of Science
Osaka University
1-1 Machikaneyama, Toyonaka, Osaka, 560-0043 (Japan)

DOI: 10.1002/adma.200904026

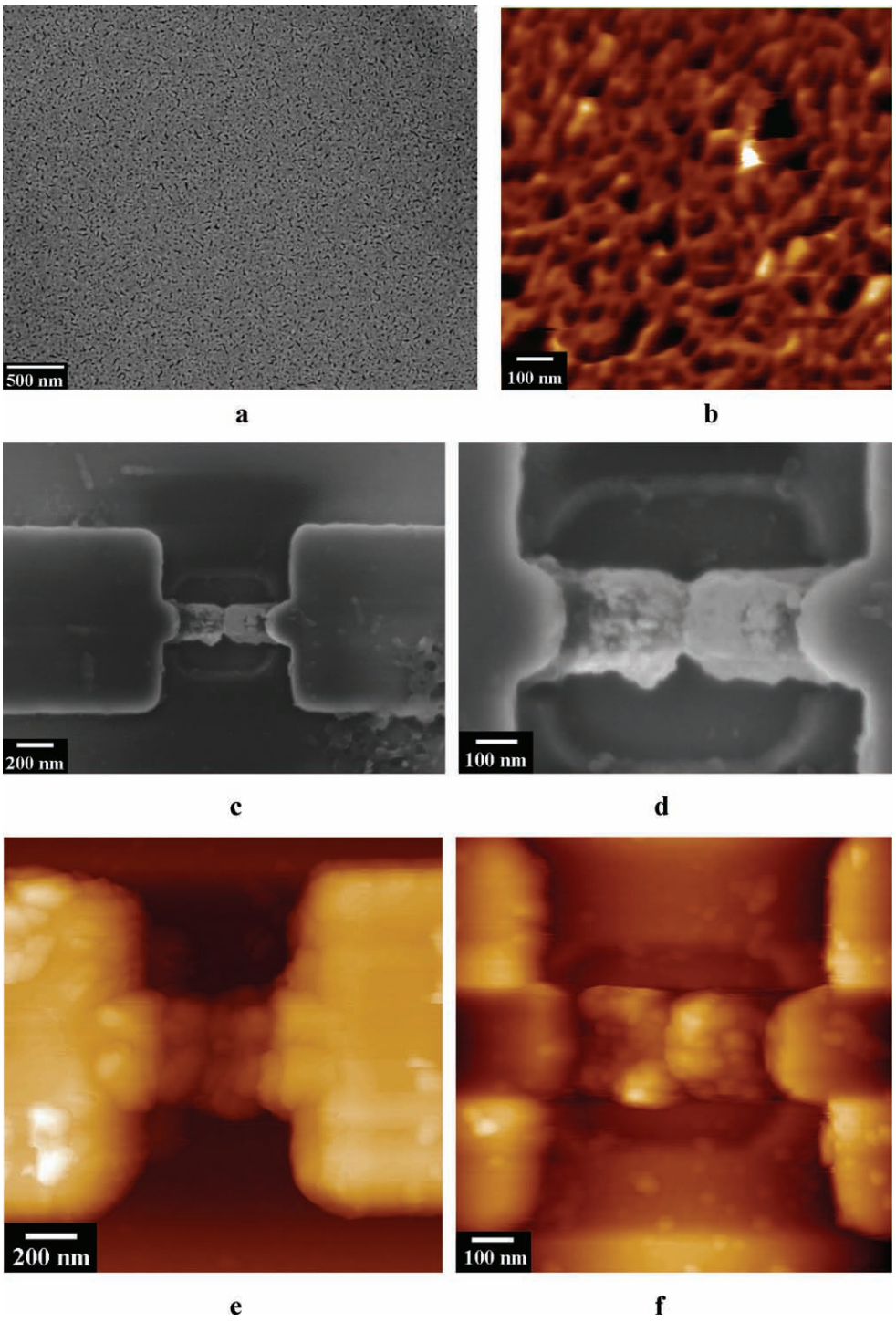

Figure 1. **a,b**) SEM and TM-AFM images for the iodine-doped sexithiophene disulfide polymer on the gold surface. **c,d**) SEM images of the nanodevice with different magnifications covered by a thick film. **e,f**) TM-AFM images for bare-nanogap-pair Au electrodes before the nanofabrication (**e**) and for the polymer covering the nanogap-pair Au electrodes (**f**).

magnifications also clearly show the formation of the sexithiophene disulfide polymer in the gap area (Figures 1c-1d). The sexithiophene disulfide polymer favors formation on the surfaces of exposed Au electrodes and bridges them by means of Au-S bonds. TM-AFM morphology observations for the nanodevice before and after nanofabrication further verified the formation of polymer in the nanogap Au electrodes (Figures 1e and 1f). An average height change of 50 nm in the gap area could be observed after nanofabrication, which is indicative of the formation of oligothiophene disulfide.

The nanodevice was further characterized by temperature-dependent current-voltage (*I-V*) measurements and reproducible *I-V* curves were recorded using a cyclic scanning mode from 8–300 K in the voltage range from –4 to 4 V with a step of 0.05 V. Full-range temperature-dependent (8–300 K) *I-V* curves of the nanodevice are shown in **Figure 2a**, in which the iodine-doped sexithiophene disulfide polymer serves as the active element. The *I-V* characteristics of this nanodevice became increasingly nonlinear with decreasing temperature. At 300 K, the *I-V* curve was almost ohmic with an average resistance of 6.88×10^6 ohm and a correlation coefficient of 0.999, which were obtained by performing a linear fit. Furthermore, the resistance of the polymer changed significantly with temperature. For example, the resistance was only 2.15×10^9 ohm at 8 K and –4 V but it was 1.63×10^6 ohm at 300 K and –4 V showing a decrease in the resistance of about 1319 times. Classical Arrhenius plots (ln*I* versus 1/*T*) were used to characterize the *I-V* behavior of this nanodevice, from which at least two different conduction mechanisms can be observed. As shown in Figure 2b, the currents in the low-temperature range were temperature-independent, as the conductance is governed only by the tunneling current. However, when the temperature increased, the contribution of the temperature-dependent thermal excitation current became dominant, making the effect of the temperature-independent tunneling current negligible. As a result, almost linear curves were obtained for temperatures higher than 120 K (Figure 2c), corresponding to the mechanism of hopping conductance.[3] The activation energy (ΔE) for this iodine-doped sexithiophene disulfide polymer based nanodevice was calculated by theoretical fits for eight curves at

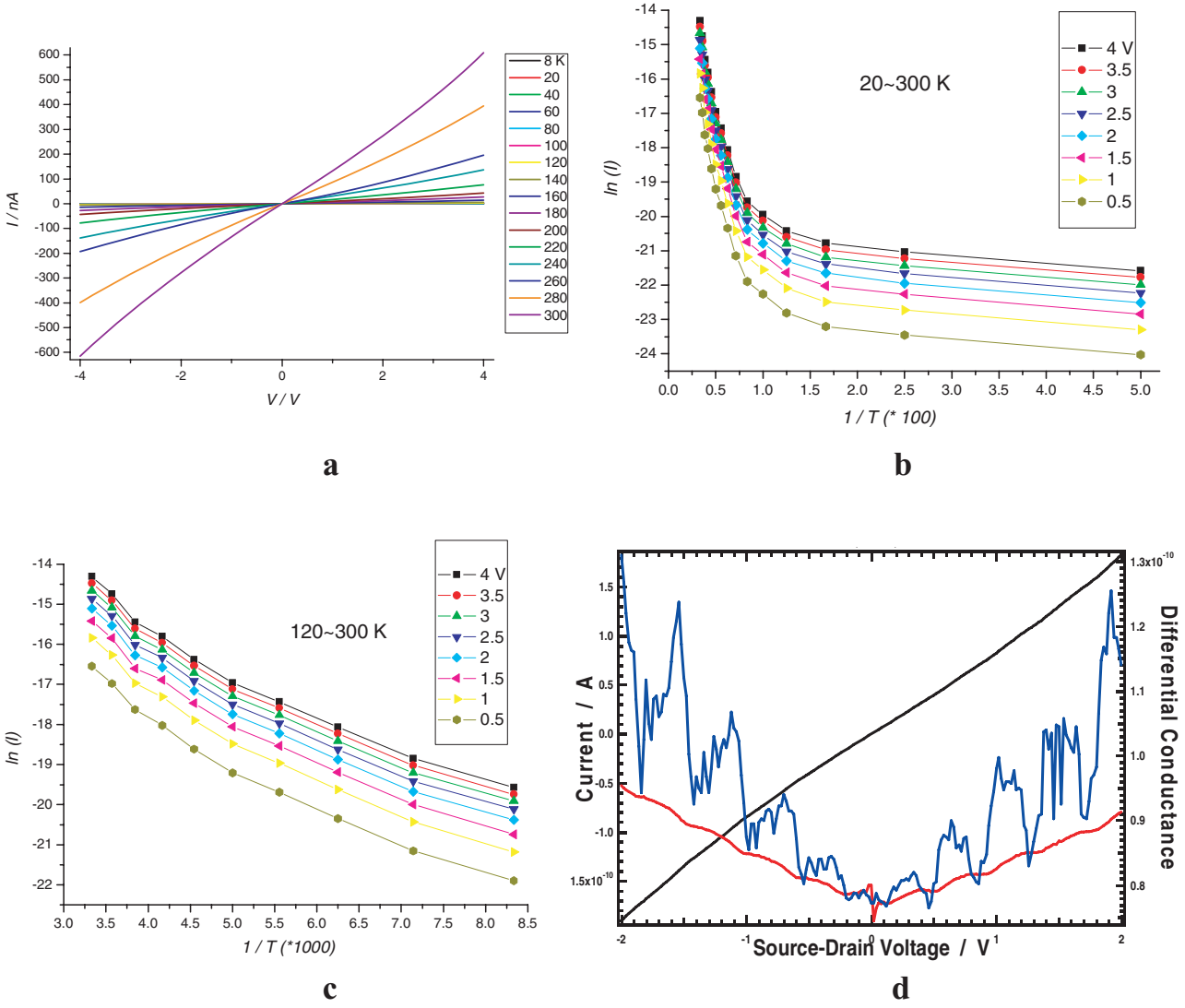

Figure 2. Temperature-dependent *I-V* characteristics of a nanodevice prepared from a 0.5 mmol L^{-1} sexithiophene solution. **a**) Full range of the *I-V* curves (8–300 K, –4 V to +4 V). **b**) Arrhenius plots at 0.5–4 V in the range of 20–300 K. **c**) Arrhenius plots for the thermal excitation current at 0.5–4 V in the range of 120–300 K. **d**) Current (black), conductance (red), and differential conductance (blue) curves for the nanodevice in the range of –2 V to +2 V with a step of 0.02 V at 8 K.

different bias voltage producing an average ΔE value of 89.6 meV in the regimes of 120–300 K and 0.5–4 V, which is comparable with those of our previously reported oligothiophene terminal dithiols/Au-NPs nanocomposite films bridging 1-μm gap gold electrodes (12–73 meV).[13,16]

It should be noted that Coulomb-blockade phenomena in this organic molecule-based nanodevice have been observed at low temperature[25,26] whereby the iodine-doped sexithiophene disulfide polymer acts as the active element for single-charge tunneling (Figure 2d). The blue differential conductance (dI/dV) curve at 8 K shows a series of continuous peaks from –6 to 6 V in our experiment with intervals of about 400 mV as the Coulomb staircase (red conductance curve), corresponding to the quantum levels of iodine-doped sexithiophene disulfide polymer (see also FigureSI2). As the typical characteristic of Coulomb blockades, these peaks diminish gradually with increasing temperature and become negligible at room temperature.

We also measure the photoresponsive properties for this nanodevice by collecting the *I-V* curves under irradiation and in dark conditions at 80, 160, and 300 K. Moreover, time-current scans were used to record the current-time (*I-T*) curves of this nanodevice at 80, 160, and 300 K at 3 or 6 V for comparison, whereby the light source was switched on and off periodically, and the temperature was controlled by an effective thermostat (liquid helium coolant). As can be seen in **Figure 3**, both *I-V* and *I-T* (the insets) plots for this nanodevice exhibit a reversible and reproducible photoresponse at different temperatures. Compared to the resistance under dark conditions (black lines),

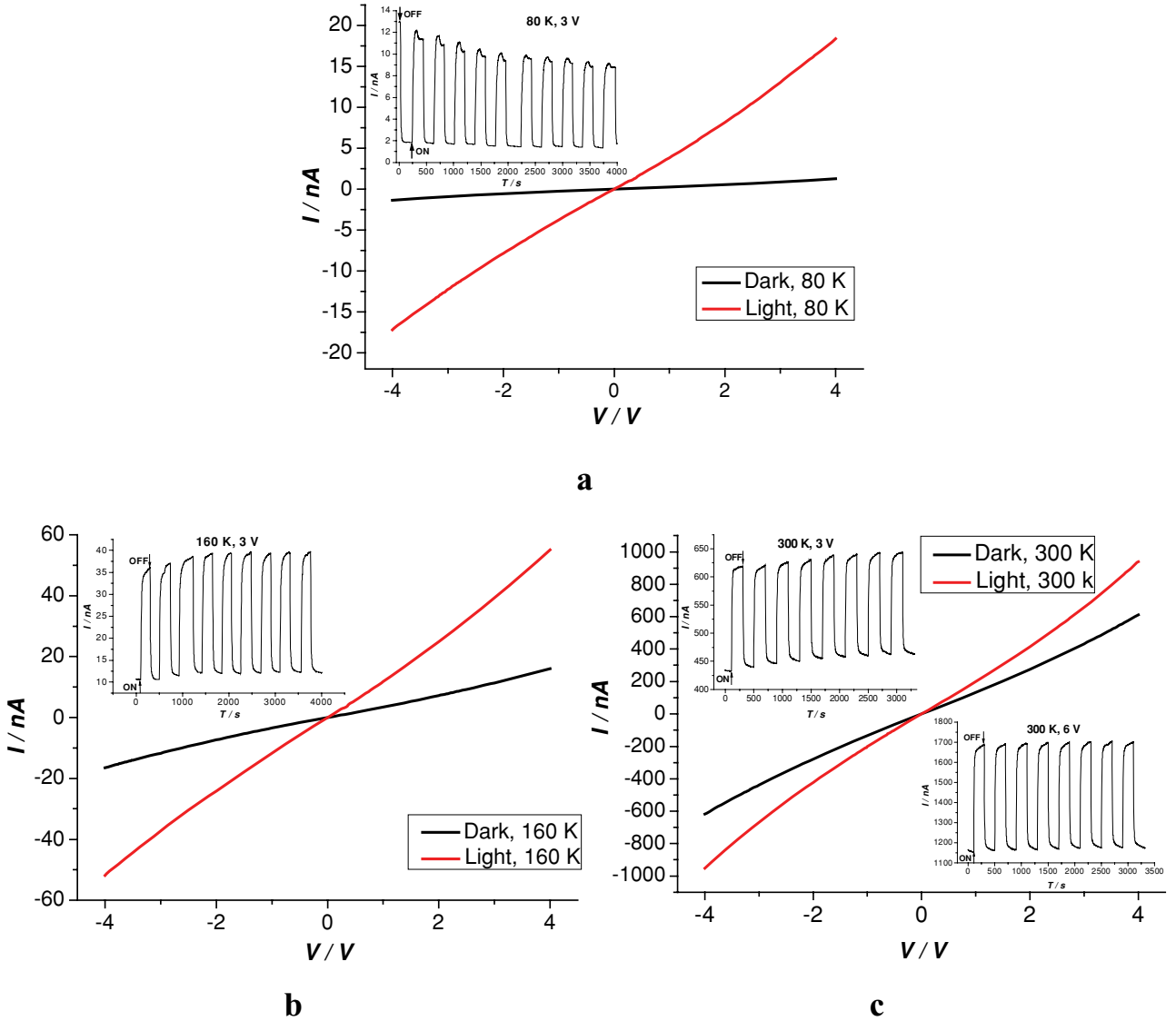

Figure 3. Reversible photoresponsive *I-V* and *I-T* curves of the nanodevice at different temperatures. **a**) *I-V* curves under irradiation (red) and in dark conditions (black) in the range –4 V to +4 V at 80 K. The inset is an *I-T* curve when the light is turned on and off periodically at 3 V, 80 K. **b,c**) *I-V* curves under irradiation (red) and in dark conditions (black) in the range –4 V to +4 V at 160 and 300 K, respectively. The inset in (**b**) is an *I-T* curve when the light is turned on and off periodically at 3 V, 160 K, whereas the insets in (**c**) are *I-T* curves when the light is turned on and off periodically at 3 and 6 V, 300 K.

the resistance at 80, 160, and 300 K is somewhat decreased under irradiation (red lines) as a result of the photogeneration of charges making the substance more conductive, which means a photoactive film is present. However, analogous to the oligothiophene-based terminal dithiols/Au-NPs self-assembled films, the degree of photoresponse depends on the temperature, whereby lower temperatures result in a higher photoresponse. The ratios of conductance (K_{light}/K_{dark}) decrease from 14.1 at 80 K to 3.3 at 160 K and 1.5 at 300 K.

When the concentration of sexithiophene was reduced to 0.1 mmol L^{-1}, thiol end-capped and iodine-doped sexithiophene disulfide polymers could still be obtained using the same experimental process. However, the resulting polymer was thin and nonlinear and low-conducting temperature-dependent *I-V* curves were recorded (see Figure SI3 for the *I-V* curves of this nanodevice). The average ΔE value for this nanodevice was 66.9 meV in the region of 160–300 K calculated by theoretical fits for eight curves at 0.5–4 V with a step of 0.5 V, whereby a decrease in resistance of only 36 times was found at 4 V in the range from 8 to 300 K.

In summary, a sexithiophene dithiol was used to fabricate iodine-doped sexithiophene disulfide semiconducting polymers bridging two facing gold electrodes with a nanogap of about 20 nm by Au-S bonds via an in-situ self-assembly method, whereby iodine simultaneously serves as an oxidant and dopant. The resulting photoresponsive nanodevices were characterized by SEM, AFM, temperature-dependent electronic conduction, and photoresponsivity measurements. Quantum effects in the Coulomb blockade were observed in the nanodevice at 8 K as the iodine-doped organic polymer serves as the active element for single-charge tunneling. Further studies on semiconducting and photoresponsive nanodevices are being undertaken in our lab in which doped oligothiophene disulfate derivatives having versatile metal-binding sites and donor-acceptor spacers act as the active elements between gap electrodes.

Experimental Section

Reagents: All reagents and solvents were of analytical grade and used without further purification. Sexithiophene terminal dithiol was prepared via the method that we have described previously.[13] The anhydrous solvents were drawn into a syringe under a flow of dry N_2 gas and were directly transferred into the reaction flask to avoid contamination. Analyses for carbon, hydrogen, and nitrogen were performed on a Perkin–Elmer 1400C analyzer. An Olympus BX60M optical microscope was used to check all the electrodes before determination of the *I-V* curves. A Yanaco Plasma Asher LTA-102 instrument was used to clean all the electrodes. SEM images were collected with a JEOL JSM-6700F microscope at an acceleration voltage of 5 KV. AFM images were recorded on a JEOL-JSPM4210 instrument. The measurements were carried out in vacuum to eliminate the influence of water adsorbed on the sample surface and increase the sensitivity and reproducibility of the experiment. The resonant frequency of the cantilevers was 250 kHz for the tapping mode.

Techniques: The details of the nanogap electrode fabrication were previously published.[27] The *I-V* curves were collected with an Advantest R6245 2 channels voltage-current source monitor interfaced to a microcomputer through a GPIB-SCSI board and NI-488.2 protocol. Data were acquired using a homemade procedure and Igor Pro 4.0 (Wavemetrics) software. The samples were mounted on top of an antivibration table in a temperature-controlled cryogenic chamber (± 0.005 °C) and the nanogap Au electrodes were used as the working and counter electrodes. All measurements were carried out in high vacuum ($P < 2.0 \times 10^{-4}$ Pascal at room temperature) formed by means of a turbo-molecular pump, and the samples were cooled using liquid helium as the coolant. The positions of the four Pt probes could be adjusted by X, Y, and Z directions in order to have them effectively touch the Au electrodes. Short triaxial cables were used to connect the nanodevices to the *I-V* monitor in order to minimize the external noise. The light source used for irradiating the samples with maximal intensity was a NPI PCS-UMX250 high-power metal halide lamp. The *I-V* curves of the photoresponse on irradiation were collected 10 min after the metal halide lamp gave maximal power. When strong light was irradiated onto the devices, the surface temperature of the devices would initially increase a little and then decrease again through thermostat control, but the temperature range of the devices only varied within 0.5 K. All the experiments were carried out at midnight in order to prevent the influence of the surrounding light.

Preparation of the Electrodes: The nanojunctions were fabricated by the self-assembly method illustrated in Scheme SI1. A freshly cleaned pair of gold electrodes with a 20-nm gap or Au-coated SiO_2 substrates were soaked in chloroform solution of sexithiophene terminal dithiol (0.5 or 0.1 mmol L^{-1}) for 30 min, and then a chloroform solution of excess iodine was added. The mixtures were kept standing for 36 h at room temperature in a glove box. The electrodes were then taken out, washed thoroughly with chloroform in order to remove excess unreacted dithiol and iodine, and dried in vacuum.

Acknowledgements

This work was supported by a Grant-in-Aid for Scientific Research (Nos. 15201028 and 14654135) and for Key-Technology, 'Atomic Switch Programmed Device' from the Ministry of Culture, Education, Science Sports, and Technology of Japan. W.H. acknowledges the Major State Basic Research Development Programs (Nos. 2007CB925101 and 2006CB806104), the National Natural Science Foundation of China (Nos. 20871065 and 20721002), and the Jiangsu Province Department of Science and Technology (No. BK2009226).

Supporting Information

Supporting information is available online from Wiley InterScience or the author.

Received: November 25, 2009
Revised: February 20, 2010
Published online: April 23, 2010

[1] A. P. H. J. Schenning, E. W. Meijer, *Chem. Commun.* **2005**, 3245.
[2] E. W. Meijer, A. P. H. J. Schenning, *Nature* **2002**, *419*, 353.
[3] M. A. Reed, T. Lee, *Molecular Nanoelectronics*, American Scientific Publishers, Los Angeles, CA **2003**.
[4] D. Fichou, *Handbook of Oligo- and Polythiophenes*, Wiley-VCH, Weinheim Germany **1999**.
[5] T. Skotheim, J. Reynolds, R. Elsenbamer, *Handbook of Conducting Polymers 2nd Edition*, Marcel Dekker, Inc., New York, NJ **1998**.
[6] M. C. Petty, M. R. Bryce, D. Bloor, *Introduction to Molecular Electronics*, Oxford University Press, New York, NJ **1991**.
[7] W. A. Schoonveld, J. Wildeman, D. Fichou, P. A. Bobbert, B. J. van Wees, T. M. Klapwijk, *Nature* **2000**, *404*, 977.
[8] A. Nitzan, M. A. Ratner, *Science* **2003**, *300*, 1384.
[9] S. R. Forrest, *Nature* **2004**, *428*, 911.
[10] S. Tan, J. Zhai, H. Fang, T. Jiu, J. Ge, Y. Li, L. Jiang, D. Zhu, *Chem. Eur. J.* **2005**, *11*, 6272.

[11] K. Araki, H. Endo, G. Masuda, T. Ogawa, *Chem. Eur. J.* **2004**, *10*, 3331.
[12] W. Huang, L. Wang, H. Tanaka, T. Ogawa, *Eur. J. Inorg. Chem.* **2009**, 1321.
[13] W. Huang, G. Masuda, S. Maeda, H. Tanaka, T. Ogawa, *Chem. Eur. J.* **2006**, *12*, 607.
[14] T. Ogawa, W. Huang, H. Tanaka, *Mol. Cryst. Liq. Cryst.* **2006**, *455*, 299.
[15] W. Huang, G. Masuda, S. Maeda, H. Tanaka, T. Hino, T. Ogawa, *Inorg. Chem.* **2008**, *47*, 468.
[16] W. Huang, H. Tanaka, T. Ogawa, *J. Phys. Chem. C* **2008**, *112*, 11513.
[17] L. Wang, W. You, W. Huang, C. Wang, X. Z. You, *Inorg. Chem.* **2009**, *48*, 4295.
[18] R. L. Carroll, C. B. Corman, *Angew. Chem. Int. Ed.* **2002**, *41*, 4378.
[19] L. Tian, C. Shi, J. Zhu, *Chem. Commun.* **2007**, 3850.
[20] G. Zotti, B. Vercelli, A. Berlin, S. Destri, M. Pasini, V. Hernandez, J. T. L. Navarrete, *Chem. Mater.* **2008**, *20*, 6847.
[21] T. K. Tran, M. Qcafrain, S. Karpe, P. Blanchard, J. Roncali, S. Lenfant, S. Godey, D. Vuillaume, *Chem. Eur. J.* **2008**, *14*, 6237.
[22] M. A. Loi, E. Da Como, F. Dinelli, M. Murgia, R. Zamboni, F. Biscarini, M. Muccini, *Nat. Mater.* **2005**, *4*, 81.
[23] M.-K. Ng, D.-C. Lee, L. P. Yu, *J. Am. Chem. Soc.* **2002**, *124*, 11862.
[24] B. Liedberg, Z. Yang, I. Engquist, M. Wirde, U. Gelius, G. Götz, P. Bäuerle, R.-M. Rummel, C. Ziegler, W. Göpel, *J. Phys. Chem. B* **1997**, *101*, 5951.
[25] H. Grabert, M. H. Devoret, *Single Charge Tunneling: Coulomb Blockade Phenomena in Nanostructures (NATO Science Series: B)*, Springer, New–York, NY **1992**.
[26] I. L. Aleiner, P. W. Brouwer, L. I. Glazman, *Phys. Rep.* **2002**, *358*, 309.
[27] K. Araki, H. Endo, H. Tanaka, T. Ogawa, *Jpn. J. Appl. Phys.* **2004**, *43* (5A), L634.